ELSEVIER

Journal of Nuclear Materials 256 (1998) 87–95

journal of nuclear materials

Characterization of corroded metallic uranium fuel plates

T.C. Totemeier *, R.G. Pahl, S.L. Hayes, S.M. Frank

Argonne National Laboratory, P.O. Box 2528, Idaho Falls, ID 83403, USA

Received 23 January 1998; accepted 27 May 1998

Abstract

A brief background on the history of the corrosion of uranium metal fuel plates from the Zero Power Physics Reactor (ZPPR) and the findings of a recent characterization of the corrosion are presented. The characterization encompassed visual examination, metallography, scanning electron microscopy, and X-ray diffraction. Corrosion of the plates has been observed essentially since their manufacture. The corrosion was found to have both general and localized forms. A black powder corrosion product associated with areas of localized attack was determined to be UH_3, while the remainder of the corrosion product was UO_{2+x}.

1. Introduction

Interest in the long-term storage properties of uranium metal has been renewed in recent years due to the extended underwater storage of metallic spent nuclear fuels (SNF) and the anticipated interim to long-term dry storage of SNF and uranium metal feedstock. Metallic SNF currently of concern in the US Department of Energy (DOE) complex include N-reactor fuel, Experimental Breeder Reactor-II (EBR-II) fuel, and Fermi reactor fuel. The principal concern with storage of uranium metal is degradation due to oxidation and corrosion during the storage period, and the possibility of forming reactive corrosion products, such as metallic fines or uranium hydride (UH_3) powder. Formation of reactive corrosion products presents safety hazards when handling the material after storage. Early anecdotal evidence on the hazards of handling improperly stored uranium was documented by Smith in 1956 [1].

Since that date, the reactions of uranium with oxygen and water vapor have been fairly extensively studied; two detailed reviews have been published by Colmenares [2,3]. Uranium reacts slowly with dry air or dry oxygen, forming an initially passive layer of slightly superstoichiometric UO_2. Diffusion of oxygen ions through the passive layer is rate controlling; cracking of the oxide at greater thickness limits its protective abilities. The reaction of uranium with water vapor also produces UO_2, according to the formula

$$U + 2H_2O \rightarrow UO_2 + 2H_2. \quad (1)$$

This reaction occurs at a much greater rate than the uranium–oxygen reaction at low temperatures. It is generally found that less than the stoichiometric amount of hydrogen gas is formed in this reaction; most researchers report the presence of UH_3 to account for the remainder of the hydrogen. The reported values of the percentages of UH_3 in the nominally oxide reaction product vary from 2 to 30 wt% of the total product [4–6]; the exact mechanism of hydride formation has not been conclusively identified. The formation of higher percentages appears to be limited to crevice-type corrosion where there is limited access of the ambient environment to the reaction product. In such a situation trapped hydrogen may react with the metal directly to form hydride.

UH_3 forms as a fine powder, is reported to be pyrophoric in the presence of air [7], and can burn at room temperature according to the relation

$$3UH_3 + \frac{25}{4}O_2 \rightarrow U_3O_8 + \frac{9}{2}H_2O. \quad (2)$$

This reaction liberates a significant amount of heat, 1490 kJ/mol UH_3. U metal fines may also be produced as a result of corrosion – these will also oxidize very rapidly

* Corresponding author. Tel.: +1-208 533 7458; fax: +1-208 533 7863.

0022-3115/98/$19.00
PII: S0022-3115(98)00448-6

at room temperature and generate heat. As uranium products are removed from enclosed storage situations where hydride and/or metal fines may have formed, exposure of the corrosion products to air may result in pyrophoric incidents, or in some cases even burning of the bulk metal itself [1].

Few reports currently exist in the literature documenting instances where hydride has been found as a corrosion product of U metal after extended storage [8]. The corrosion in storage of highly-enriched uranium (HEU) fuel plates manufactured for use in the Zero Power Physics Reactor (ZPPR) at Argonne National Laboratory (ANL) provides one such example. These plates are coupons of HEU clad in stainless steel; crevice corrosion of the plates has occurred since they were originally clad in 1982. A detailed characterization of the plates and their corrosion products is currently being performed to gain a better understanding of the nature of uranium corrosion.

This paper presents a brief background of the ZPPR fuel plate corrosion problem and the results of an initial characterization of the corrosion and products. The background describing the history of the ZPPR fuel plate corrosion problem is first presented. The findings of a recent characterization of the corrosion using visual examination, metallography, scanning electron microscopy (SEM), and X-ray diffraction (XRD) are then described, followed by a discussion of the potential factors contributing to the severity of the corrosion and the high UH_3 contents present in the corrosion products.

2. Background

The Zero Power Physics Reactor (ZPPR – originally termed the Zero Power Plutonium Reactor) began operation in 1969. It was built to provide a testbed for fast-critical assembly reactor physics experiments in support of advanced fast reactor designs, and was the culmination of a series of fast critical facilities – Zero Power Reactor (ZPR)-3, ZPR-6, and ZPR-9. Most ZPPR fuel elements were stainless steel drawer-type containers that were loaded with rectangular pieces of reactor materials; many types of materials were available for use, including high enriched uranium (HEU) metal. The fuel has essentially zero burnup due to the extremely low power nature of the reactor.

The HEU plates used in the ZPPR reactor were originally manufactured for use in the earlier ZPR reactors. The manufacture of the first HEU plates for use in ZPR-3 was described in 1955 by Yaggee [9]. These plates were 7.6 cm by 5.1 cm by 3.2 mm in dimension, and were produced by hot rolling cast billets of uranium. The rolled sheet was sheared, stamped, and machined to close final dimensional tolerances.

All of the ZPPR plates originally were coated with a non-hydrogenous, organic polymer coating, $(C_2F_3Cl)_n$, commonly referred to as KEL-F. This coating was applied to prevent spread of contamination, and to retard oxidation of the plates during their exposure to the ambient environment. Apparently this coating was not fully effective in preventing oxidation, as the plates – some described as 'badly oxidized' – were re-coated in 1969. In 1981, the decision was made to remove the KEL-F coating and place the plates into stainless-steel cladding. The prime motivation for use of a cladding was containment of alpha contamination.

The cladding operation was performed from February 1982 through January 1983. The stainless steel cladding was sealed at each end by a porous metal frit end plug. The porous end plugs were specifically chosen to allow any residual organic vapors to escape from inside the cladding and to allow the plates to 'breathe'. Subsequent experience revealed this decision to only worsen the corrosion problem by allowing access of gaseous reactants (such as H_2O) to the U metal.

At this point, the terminology that will be used to describe the plates should be clarified. For the purposes of this paper, 'coupon' will refer to the rectangular HEU metal pieces themselves, while 'plate' will refer to a stainless-steel clad assembly of one or more 'coupons'. Fig. 1 is a schematic diagram showing a clad assembly of plates. As described above, as-manufactured coupons came in different lengths and thickness; all coupons were 51 mm wide. The two available lengths were 51 mm and 76 mm; 3.2 mm and 1.6 mm thicknesses were available. These coupons were assembled into clad plates with lengths varying from 51 mm to 200 mm. The plates have been, and are currently, stored in rectangular aluminum overpack canisters which have rubber gasket seals.

Corrosion of the clad HEU plates in the form of cladding bulging was first noticed in 1985, only three years after the cladding operation. To determine the nature of the corrosion, four defect plates were examined. The plates were declad in an air hood, and when the cladding was peeled back from a particularly bulged area of one plate, a strong flash was observed. X-ray diffraction of corrosion products from the four plates showed the presence of UO_2, both α and β forms of UH_3, and UN. The observation of pyrophoric events during decladding was linked to the presence of UH_3 in the corrosion product.

The first remedial action to inhibit the corrosion was to place bags of anhydrous $Mg(ClO_4)_2$ desiccant in the overpack canisters with the plates. The desiccant was intended to remove moisture from the ambient atmosphere in which the plates were stored. In 1990, however, continued corrosion was observed. The anhydrous $Mg(ClO_4)_2$ apparently did not act as an effective desiccant because of the reversibility of $Mg(ClO_4)_2$

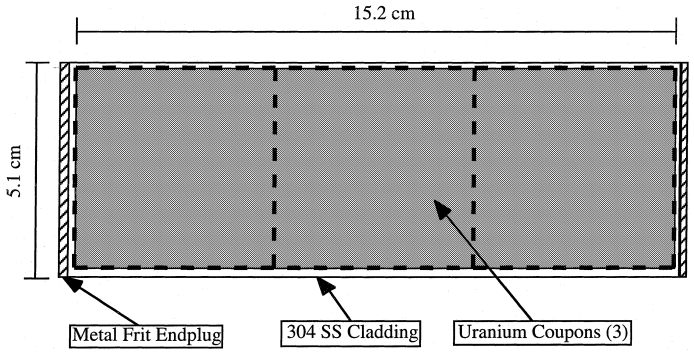

Fig. 1. Schematic diagram of ZPPR plate and coupons.

hydration. A second attempt to halt corrosion was made by evacuating the overpack canisters.

Unfortunately, the canisters were not originally designed for evacuation; the upper and lower halves of the canister were joined by only two bolts, one at each end. Most canisters leaked sufficiently to allow a return to atmospheric pressure fairly quickly. Cycles of evacuation, in-leakage, and re-evacuation only exacerbated the corrosion problem. When air leaked into a canister, O_2 and H_2O reacted with U in the plates, the final canister environment being mostly nitrogen at nearly atmospheric pressure. At that point oxidation of the plates should have essentially stopped, although, as discussed below, diffusion of H_2O and O_2 through the elastomer seal would still have occurred.

The cycle of continuing corrosion was confirmed in 1992 by analysis of the gas present in the canisters about a year after evacuation [10]. Five canisters were studied: two containing plates already rejected by excessive bulging, and three containing what were considered to be 'good' plates. The pressure in four of the five canisters was nearly at atmospheric levels, confirming that leakage had occurred. The pressure in the fifth canister was approximately one-third of atmospheric. The O_2 content in all canisters had been reduced to less than one volume percent, and H_2 levels were high, ranging from 0.16 vol.% to 13.34 vol.%. The conclusion was that oxidation by O_2 and H_2O had occurred, even in canisters with good plates.

As a result of these findings, evacuation of the canisters was discontinued. A second getter system was chosen for use which consisted of a packet containing unsaturated hydrocarbon with a palladium catalyst and lithium hydride. The hydrocarbon is 1,4-bis (phenylethynyl) benzene (referred to as 'DEB'), which contains two carbon–carbon triple bonds. The getter system removes H_2, H_2O, and O_2. This system has apparently been effective. The gas in several canisters was initially sampled monthly and checked for O_2 and H_2. No concentrations in excess of 0.1% percent were observed. In addition, yearly inspection of the canisters containing non-corroded plates has revealed no additional corrosion since the use of the getters. Unfortunately, through the course of the 12-year time period from the cladding operation to the use of getters, over 25% of the total plate inventory underwent sufficient corrosion to be reject, an amount which corresponds to over 2000 plates.

In 1995 the US Department of Energy approached ANL-W to obtain HEU from the corroded ZPPR plates for production of research reactor fuel. A procedure for separation of useful metal from the cladding and corrosion products was proposed and implemented. The procedure entailed decladding of the plates in an inert atmosphere glovebox, separation of loose corrosion products from the metal coupons, 'passivation' of the separated corrosion products by grinding and exposure to an Ar–3%O_2 environment, and casting of the metal coupons in an induction furnace. Approximately 1200 plates with about 376 kg of HEU have been processed using this procedure. No pyrophoric incidents occurred during execution of the procedure, however, an event did occur in March 1998 during handling of the 'passivated' powders after extended vault storage. This event is currently being investigated and no further plates have been processed.

3. Characterization procedures

During the recent period of processing, plates were examined to better understand the nature of the corrosion and corrosion products. Many plates were visually inspected as they were declad during processing; the extent and morphology of corrosion were noted. Photographs were taken of typical plates, corroded metal coupons, and corrosion products. Metallographic cross-sections of three corroded coupons were prepared to investigate the relationship between coupon microstructure and corrosion. The first coupon was severely corroded, the second showed moderate localized corrosion, and the third did not show any localized corrosion

but some general surface oxidation. Cross-sections of the coupons were prepared using standard metallographic techniques and examined using a light microscope.

Loose corrosion products found upon decladding the plates were examined both visually and using scanning electron microscopy (SEM). SEM examination was performed on samples of the loose corrosion products from two plates – plate 2652, which was badly corroded, and plate 2249, which was relatively intact. The degree of corrosion for all plates was qualitatively assessed by the relative extent of cladding bulging. The corrosion product samples were loaded onto carbon sticky pads in an inert atmosphere glovebox and coated with palladium prior to examination. Examination was performed using a ISI SS40 SEM operating at 20 kV.

X-ray diffraction (XRD) was used for identification of phases present in the loose corrosion products. XRD analysis was performed on samples from four plates, plates 2652, 2249, 4042, and 4414. Plates 2652 and 2249 are mentioned above. Plate 4042 was badly corroded, and plate 4414 showed little sign of corrosion. The samples analyzed were believed to be representative of the loose corrosion product in a given plate. To achieve this, the loose corrosion products from each plate were collected and stirred to a uniform mixture, and samples were taken of the mixture. XRD was also performed on small samples of the two forms of corrosion product observed, flake and powder. These two forms are described in Section 4.2. All samples were crushed to a fine powder in a high-purity Ar glovebox and then loaded into a sealed environmental chamber. Diffraction was performed on a Scintag X1 powder diffractometer using Cu K-alpha radiation. The scan range was from 20° to 100° 2θ with a scan rate of 0.75° per minute. The diffraction patterns obtained were analyzed using Sietronics standardless quantitative XRD phase analysis software.

4. Results

4.1. Corrosion morphology

Corrosion of the U coupons manifested itself in the clad plates as extensive bulging of the cladding. Fig. 2 shows a single plate (3606) with extensive cladding deformation along the two long edges of the plate. The inset close-up in Fig. 2 shows a significant breach which has resulted from excessive cladding deformation. The bulges were most commonly found along the edges of the cladding, rather than in the center. Severe localized corrosion attack was correspondingly found to initiate along the edges of the uranium coupons, as described below. The cladding itself showed no sign of corrosion attack; breaching of the cladding appears to have been solely due to the volume expansion of the corrosion product relative to the parent metal. For transformation of U metal to UO_2 a minimum expansion of 72% occurs. A wide range of cladding bulging was observed. Some plates showed very little sign of bulging, while others were grossly deformed with more than one cladding breach.

The severe corrosion of the U coupons was clearly observed upon de-cladding of the plates. Loose powder and dust quickly spread throughout the glovebox during the decladding operation. Figs. 3 and 4 show coupons immediately following cladding removal. Fig. 3 is an archival photo from 1985, and Fig. 4 is a recent photo showing coupons from the bulged plate of Fig. 2. A clear difference between the two sets of coupons was the extent of general corrosion. The coupons in Fig. 4 showed a large amount of general corrosion which was manifest in the form of gray flakes and fine dust. Much of the gross corrosion product was removed from these coupons before they were photographed. In contrast, little general corrosion was observed for the coupons in Fig. 3; especially for the two coupons on the left side.

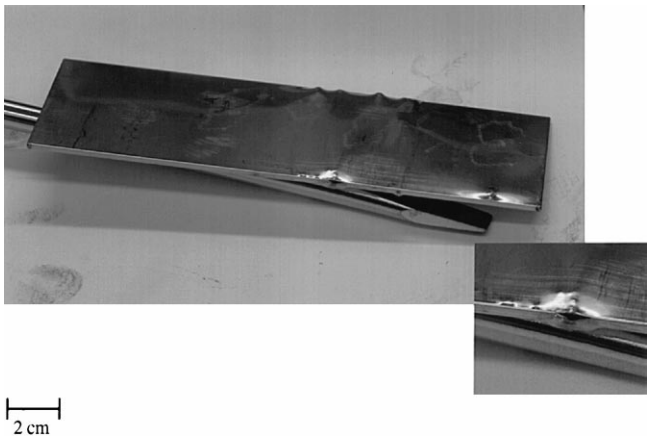

Fig. 2. Bulged ZPPR plate (3606); inset shows close-up of cladding breach.

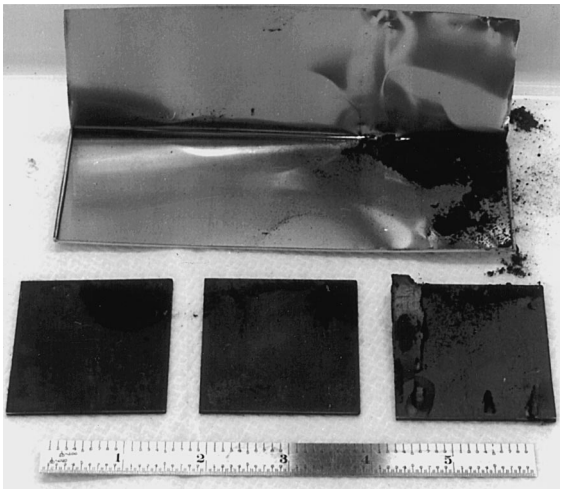

Fig. 3. Declad ZPPR plate showing localized corrosion of right coupon (1985 examination).

A second form of corrosion observed was more severe and localized. This type of corrosion is clearly shown on the right hand coupon in Fig. 3 and the top coupon in Fig. 4. This form of corrosion had several notable characteristics. First, localized corrosion was almost always observed on only a single coupon for each plate (a plate contains two or three coupons). The corrosion appeared to have initiated at the transverse edges of the coupons, and often took the form of blistering or transverse cracking. The right hand coupon in Fig. 3 shows lifting of metal due to sub-surface cracking and attack. Cracking and blistering were most commonly observed at early stages of corrosion (judging on the basis of overall attack). For more severely corroded coupons the localized attack consumed large areas of the coupon. The top coupon in Fig. 4 is a good example, with large quantities of material missing from its edges. There was no consistent location of localized corrosion, i.e. it did not occur in any particular place, such as near the metal frit endplugs.

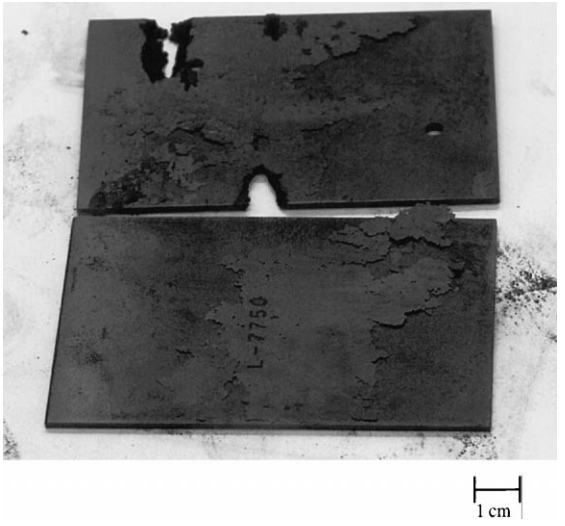

Fig. 4. Coupons from plate in Fig. 2 showing severe local and general corrosion.

4.2. Coupon microstructure

The above characteristics suggest that the localized corrosion may be microstructurally related since the corrosion appeared to initiate on the coupon edges. The microstructures of three plates were examined to determine if such a link exists. Due to the thickness of oxide on the coupons, all three proved difficult to polish. During final polishing, oxide particles tended to separate themselves from the plates and scratch the metal surface. The two coupons which had localized corrosion showed interior cracking along their longitudinal axes, as shown in Fig. 5. The severely corroded coupon had many more cracks than the moderately corrosion coupon, and the coupon with localized corrosion did not show any interior cracking. Unfortunately, no distinct microstructural features were identified which could account for the apparent increased susceptibility of some coupons to localized corrosion compared to others. Although the grains visible in Fig. 5 are slightly elongated in the rolling direction, no highly elongated grains or oriented inclusions were observed in the coupons with localized corrosion. Slightly elongated grains were also observed in the coupon which did not show localized corrosion.

4.3. Corrosion products

The corrosion products analyzed in detail were loose products, i.e. those which were removed from the coupons by light brushing. Such brushing left a dark gray adherent product on the metal surface, which was

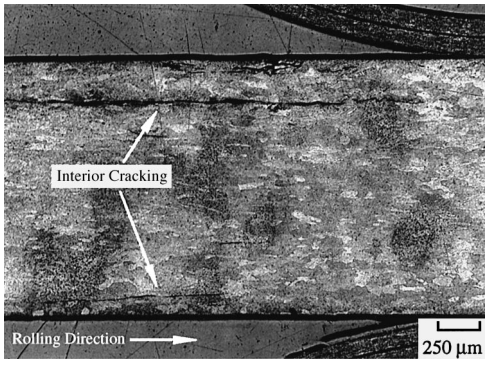

Fig. 5. Metallographic cross-section of coupon from plate 3401 showing interior cracking and equiaxed grains.

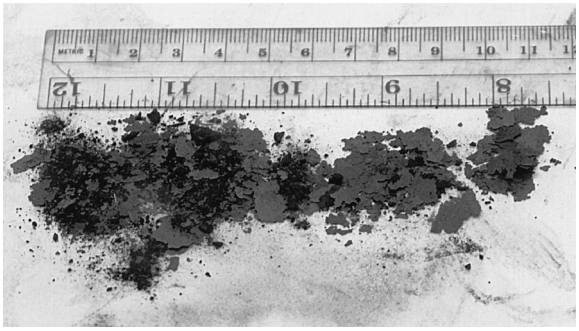

Fig. 6. Loose flake and powder corrosion product from plate shown in Fig. 2.

assumed to be oxide. The loose products were composed of two distinctly different types – a light gray, flake-like material, and a black powder. Fig. 6 is a photograph of the loose products obtained from the plate in Fig. 2. For this plate, which was considered to be relatively badly corroded, there were approximately equal amounts of flake and powder. Some of the powder was found agglomerated into fairly large chunks one or two millimeters in size. These chunks could be easily broken into powder. The quantity of powder appeared to be dependent on the extent of localized corrosion. The corrosion products from plates which did not show severe bulging and localized corrosion were composed nearly entirely of flake material.

X-ray diffraction patterns from samples of flake and powder material in the 2θ range from 20° to 60° are shown in Fig. 7. The powder material was found to have strong β-UH_3 peaks, with a small peaks of either UO_2, U_3O_7 (UO_{2+x}), or a mixture of both. Both types of uranium oxide had a good match with the diffraction pattern. Due to the width of the peaks it was not possible to differentiate between the two. In contrast, the flake material showed strong peaks from the oxide and only minor hydride peaks.

The diffraction patterns of the samples taken from plates 2249, 2652, 4042, and 4414 also showed oxide and hydride peaks. The results of the standardless quantitative analysis of the patterns for the four samples are given in Table 1. Samples from plates showing little corrosion (2249 and 4414) had no or very little hydride, while the samples from the highly corroded plates (2652 and 4042) had significant hydride contents.

SEM examination of the loose corrosion products from plates 2249 and 2652 revealed marked differences between them. Figs. 8 and 9 show images of the products from the two plates at equivalent magnifications. The sample from plate 2249 was comprised of relatively large plate-like particles of sizes varying from nearly a millimeter to tens of microns. The platelets shown in Fig. 8 are approximately 150 μm in size. The thickness of the platelets could not be determined. In contrast, the sample from plate 2652 was comprised of some platelets along with a considerable fraction of finer particles (Fig. 9). Fig. 10 shows a higher magnification

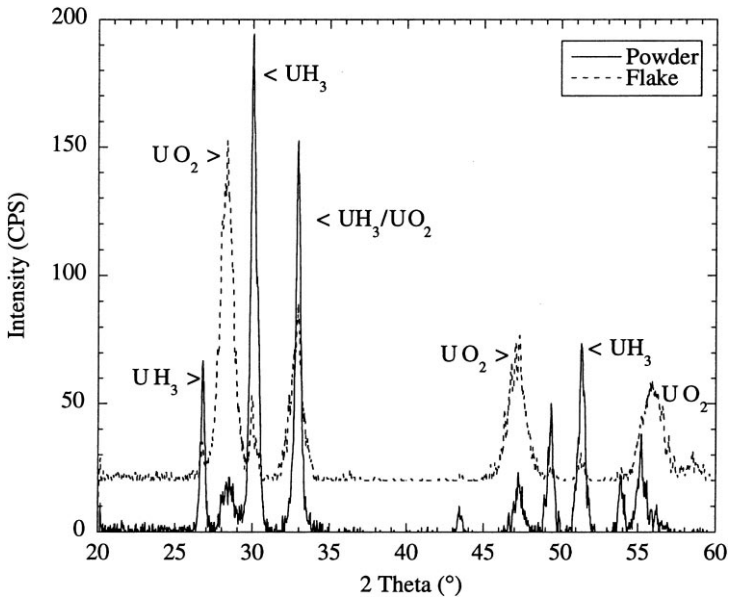

Fig. 7. XRD patterns from flake and powder corrosion products. Only major peaks are labeled; unlabeled peaks in the powder trace are from UH_3.

Table 1
Semi-quantitative XRD diffraction results from loose ZPPR fuel corrosion products

Plate ID	UH_3 (wt%)	UO_{2+x} (wt%)	Relative corrosion extent
2249	5	95	Light
2652	50	50	Severe
4042	85	15	Severe
4414	0	100	Light

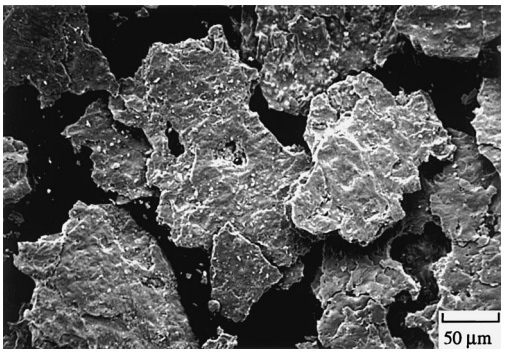

Fig. 8. SEM micrograph of plate 2249 corrosion product.

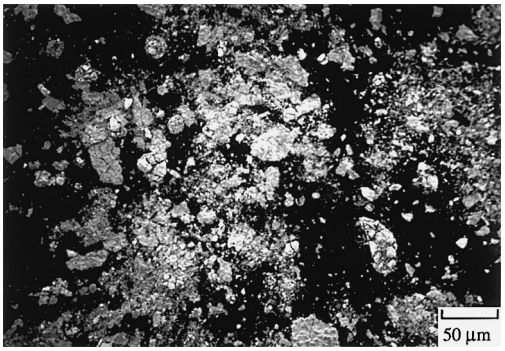

Fig. 9. SEM micrograph of plate 2652 corrosion product.

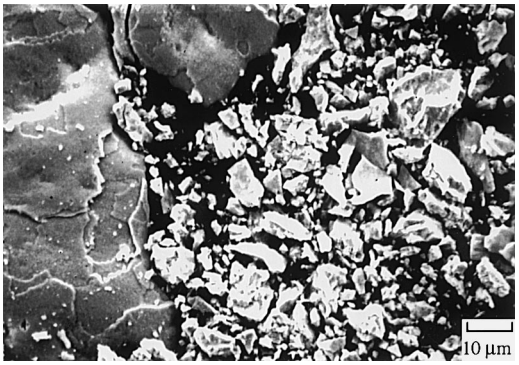

Fig. 10. Higher magnification SEM micrograph of plate 2652 corrosion product.

image of the fine particles next to a larger platelet. The sizes of the fine particles ranged from less than a micron to approximately 10 μm. The different types of product, platelets and fine particles, are believed to correspond to the flake and powder observed visually – the large plates are uranium oxide, and the fine particles are hydride. This has not been confirmed directly; the energy-dispersive X-ray spectrometer available does not permit analysis for oxygen or hydrogen.

5. Discussion

The ZPPR fuel plates are one example of U corrosion resulting in the creation of products containing high concentrations of UH_3. Because of the current sensitivity of this subject, it is important to attempt to understand the causes of the corrosion, both initially and continuing, and the means by which UH_3 was created in such large quantities. The root cause for the severe corrosion appears to be the crevice-producing effects of the tight fitting cladding and the use of metal frit endplugs which allowed access of a corrosive atmosphere to the coupons. If the metal coupons had been hermetically sealed into the cladding jackets, very little corrosion would have occurred because the reactant would be limited to the small amount of gas present in the free space inside the cladding. Severe localized corrosion also would not have been expected had the coupons been left exposed to ambient air without a jacket. The experience with the coupons prior to cladding supports this statement. General oxidation was observed, but not severe localized corrosion.

Based on the results of the 1985 examination, the corrosion began soon after the coupons were clad. It was speculated at that time that the initiator for the localized corrosion was water adsorbed onto the coupons just prior to their insertion into the cladding jackets. The cladding operation was performed in an air environment, and all of the plates found to be badly corroded in 1985 were clad in the early summer of 1982, likely a period of high humidity. Water was postulated to have entered into rolling-related cracks on the transverse faces of the coupon, thereby initiating a cycle of localized attack. In this scenario the formation of UH_3 in the initial reaction of the adsorbed water with U causes the UO_2 also formed to be non-protective, leading to continued accelerated attack in the area. The formation of UH_3 in the reaction of U with H_2O was linked to accelerated oxidation rates by Kondo et al. [4]. Recent results obtained by Moreno et al. [11] indicate that UH_3 tends to initially form at crystallographic irregularities such as grain boundaries and twins. Hence, the observation of localized attack in the ZPPR coupons primarily on the ends of the rolled plates need not be dependent on the presence of edge cracks, but

could be simply related to the increased density of grain boundaries on the transverse sections relative to the longitudinal faces.

The continuing corrosion is certainly related to access of the ambient storage environment to the plates and coupons. The gas within the aluminum overpack canister would provide an initial source of oxygen and water vapor, however this amount alone cannot account for the extent of corrosion observed. There are several mechanisms for gases to enter the canister. Simple opening of the canister to use the plates or to perform accountability checks will renew the gases. Another mechanism is 'breathing' of the canister due to varying atmospheric pressure over time. The varying pressure differential provides a driving force for exchange of gases through a non-hermetic seal. Evacuation of the canister, as implemented for several years, provides a strong driving force for in-leakage of gases. Finally, simple permeation of O_2 and H_2O through the elastomer seal can occur even at equilibrated pressure. All of the above routes would provide additional reactants to sustain the corrosion.

The high UH_3 concentrations in the loose corrosion product for some of the plates and the observation of H_2 gas in the canisters strongly suggests that the reaction of the coupons is primarily with H_2O rather than O_2. This observation further implies that H_2O has preferential access to the plates. The reaction of U with a mixture of H_2O and O_2 (i.e. humid air) does not produce H_2 gas. Only when O_2 levels are less than approximately 100 ppm does the reaction produce H_2 and UH_3 [3]. One possible mechanism by which this could occur is preferential permeation of H_2O through the elastomer seal. Permeation rates of H_2O through polymers are much greater than those of oxygen [12]. In this scenario, the U metal reacts first with O_2 originally present in the canister and then H_2O. H_2O then preferentially enters the canister through permeation and continues the react with the metal, creating H_2 gas and UH_3. The entrapment of H_2 gas in the canister likely promotes UH_3 formation. The crevices of areas of localized corrosion also will tend to trap hydrogen and promote UH_3 formation. The formation of UH_3 in crevice corrosion of U with H_2O has been documented [13].

The results of the XRD and visual observations of corrosion indicate that UH_3 is associated with areas of localized corrosion. Plates for which severe localized corrosion was not observed contained very little or no detectable UH_3. It is unclear why some plates had localized corrosion and some did not. Because localized corrosion tended to be associated with only a single coupon within a plate, it seems likely that the coupons which showed localized corrosion are different in a way that would render them more susceptible to attack. The metallurgical examination, however, did not reveal any obvious microstructural differences between severely corroded coupons and those which were relatively unaffected. It is possible that a difference exists that was not discovered in the inital examination. Another possibility is that only certain coupons retained sufficient adsorbed H_2O during the cladding operation to initiate localized corrosion. Additional characterization and testing is required to resolve this issue.

6. Conclusions

This paper summarized the past experience at ANL-W with uranium metal ZPPR fuel plates and presented the results of a recent characterization of the corrosion morphology and products. The ZPPR plates have a long history of corrosion problems, which became more serious following cladding of the plates using porous metal endplugs. The corrosion was found to have both general and localized forms. The localized attack originated on the transverse faces of the rolled uranium metal coupons. A black powder corrosion product associated with the areas of localized attack was determined to be UH_3, while the more general flake-like product was UO_2 or UO_{2+x}.

Acknowledgements

The authors wish to acknowledge the following people for assistance with obtaining background information and characterization of the plates: J.R. Krsul, E.L. Wood, H.F. McFarlane, R.J. Briggs, and D.C. Crawford. This work was supported through funding by the US Department of Energy, Reactor Systems, Development and Technology, under contract W-31-109-Eng-38, and by the US Department of Energy National Spent Nuclear Fuel Program.

References

[1] R.B. Smith, The fire properties of metallic uranium, TID-8011, Technical Information Service – Atomic Energy Commission, Wahington DC, 1956.
[2] C.A. Colmenares, Prog. Solid State Chem. 9 (1975) 139.
[3] C.A. Colmenares, Prog. Solid State Chem. 15 (1984) 257.
[4] T. Kondo, F.H. Beck, M.G. Fontana, Corrosion 30 (1974) 330.
[5] M.M. Baker, L.N. Less, S. Orman, Trans. Faraday Soc. 62 (1966) 2513.
[6] K. Winer, C.A. Colmenares, R.L. Smith, F. Wooten, Surf. Sci. 183 (1987) 67.
[7] J.J. Katz, E. Rabinowitch, The Chemistry of Uranium – Part I, McGraw-Hill, New York, 1951.
[8] S.C. Marschman, T.D. Pyecha, J. Abrefah, Metallographic examination of damaged N reactor spent nuclear fuel

element SFEC5, 4378, Pacific Northwest National Laboratory Report PNNL-11438, 1997.
[9] F.L. Yaggee, The manufacture of enriched ZPR-III fuel plates, Argonne National Laboratory Report ANL-5599, 1956.
[10] C.W. Solbrig, J.R. Krsul, D.N. Olsen, in DOE Spent Nuclear Fuel – Challenges and Initiatives, Salt Lake City, UT, 13–16 December, ANS, La Grange Park, IL, 1994.
[11] D. Moreno, R. Arkush, S. Zalkind, N. Shamir, J. Nucl. Mater. 230 (1996) 181.
[12] H. Yasuda, V. Stannett, in: J. Brandrup, E.H. Immergut (Eds.), Polymer Handbook, Wiley, New York, 1975.
[13] V.H. Troutner, Mechanisms and kinetics of uranium corrosion and uranium core fuel element ruptures in water and steam, Hanford Atomic Products Operation Report HW-67370, 1960.